

Subjects identification using ECG and PPG signals recorded from user-friendly devices

Lucia Depaoli[†], Simone Mistrali[‡]

Abstract—Electrocardiogram (ECG) and photoplethysmogram (PPG) signals have caught researchers attention recently, for a various amount of reasons. A part from the medical one, these signals can be used in biometric authentication and biometric identification in order to achieve high level of security, allowing the users to stop relying on traditional procedure such as passwords or PINs, which can be easily broken down by cyberattacks.

In this work, starting from two user-friendly devices that can records these signals, we construct two datasets. The first one is made up by data taken from 4 different subjects, while the second one data from 2 subjects, both at rest and in motion. Using different algorithm and CNN architectures, we managed to correctly classify the subjects and the motion, reaching an accuracy on the test set of about 99% for the ECG signal and 90% for the PPG signal.

Index Terms—Biometric Identification, Classification, Supervised Learning, Signal Preprocessing, SVM, KNN, CNN.

I. INTRODUCTION

Nowadays, electrocardiogram (ECG) and photoplethysmogram (PPG) sensors are becoming more and more used from people in their everyday life. They can be found in smartphones, smartwatches or fitness trackers such as chest strap or pulse oximeter. Usually these devices continuously record data from the owner, making them eligible for medical reason, for example by keeping track of the pressure or heartbeat during exercises and predict a possible anomaly, or for security application, such as biometric authentication or subject identification.

Biometric authentication is already present in our smartphones (fingerprints, face recognition), but it is probably that, in the future, it will completely replace the historic authentication tools, such as passwords or PINs, mostly due to safety reasons. PPG and ECG signals are indeed impossible to forget and difficult to being stolen comparing with knowledge and object-based method [1]. Also, continuous authentication is implementable and preferable [2]. The difference between biometric and traditional authentication is that, in the first case, the output is not Boolean, but it is a confidence interval [3]. Therefore the task is to find a way to determine, with the highest level of accuracy possible, whether the person is the actual user or a stranger (authentication procedure) or which one of the users she is (identification procedure). Most of works are about the first task [1] [3] [4] [5] [6], whereas little study is done on the second one.

In our work we try to investigate the accuracy we can reach in subject identification using biometric data. By collecting ECG and PPG signals from different persons and in different conditions, we construct two datasets. After a preprocessing operation and a first look at the data, a preliminary classification using k-Nearest Neighbor (k-NN) and Support Vector Machine (SVM) algorithms is done, evaluating the performance. Finally, different Neural Network (NN) architectures are used. The results achieved reach high accuracy and have small computational time, making the devices and the networks suitable for real time application. Outcome using a principal component analysis (PCA) projection of the data onto a less-dimensional space is also investigated.

To summarize, the main contributions we have achieved are:

- We construct two different datasets using user-friendly devices that do not require other than a smartphone to being recorded.
- We perform a subject identification using basic tools with small computational time, such as k-NN, SVM and CNN with a small number of parameters.
- We project the data onto a less-dimensional space using PCA algorithm, reducing the time complexity, and still being able to reach high accuracy in the task.

II. RELATED WORK

Most of the works about biometric signals for authentication make use of PPG signal, because it is more easy to acquire than ECG signal. Indeed, ECG based authentication reaches higher accuracy score, but it is not widely used because it is more inconvenience and invasive, since chest strap or electrodes must be put over the user body.

Often signals are processed in a way to create datasets made by multifeature [5], fiducial points or statistical information such as systolic peak, diastolic peak, heart rate variability [1], extrapolated from the PPG signal. This leads to less dimensional samples respect to the one we have used in our work. Using this approach, the Euclidean distance is not optimal since it have the limitation of the susceptibility of different features scales in the vector. The problem is solved by replacing it with the Mahalanobis distance [1]. In this case, for the classification task, algorithms such as linear discriminant analysis (LDA), quadratic discriminant analysis (QDA) [4], Naive Bayes Classifier [5], k-NN, SVM [7], Random Forest (RF) [2] are used. A classification approach using CNN is recent, but promising: since PPG signal have a time dimensionality, some research have recently implemented

[†]Department of Physics, University of Padova, email: {lucia.depaoli.1}@studenti.unipd.it

[‡]Department of Physics, University of Padova, email: {simone.mistrali}@studenti.unipd.it

long short-term memory (LSTM) after the CNN architecture, reaching optimal results in terms of accuracy [8] [9].

An important improvement in the preprocessing of the PPG signal is done in [4], which solve the problem of the alignment and matching between any two pulses. In this work, each sample is preprocessed using a limit cycle and angle-based alignment. That make each samples similar to the others. Then, using LDA and QDA as classifier, an accuracy between 90% and 95% is reached.

ECG classification can be the future of subject identification because of its similarities with the DNA, such as the universality and distinguishability: every animals with an heart can produce it and there are not two identical DNA or ECG signals in the world [10]. Given these characteristics and its consistency, ECG signal can be classified using a 1-D CNN that can automatically extract the features, making useless to rely on an expert to do it, so the raw (or at least filtered) signal can be used [11]. On the other hand, many studies use a multi-step classification, ECG signal is pre-processed in order to extract different features such as Short-time Fourier Transform (STFT), Continuous Wavelet Transform (CWT), Principal Components analysis (PCA) or the variance and energy of the wavelet coefficients, such as the R-R ratio for consecutive ECG beats [12] [13] [14]. As for the PPG signals, also in this case many research uses different classification algorithm such as SVM [15] [14], k-NN and Random Forest [16].

III. PROCESSING PIPELINE

The work is structured as follows: in Sec. IV are presented the main tools we used for preprocessing, data visualization and classification tasks. In Sec. V the CNN architectures are explained. In Sec. VI are shown the devices' characteristics and the type of data we are dealing with. In Sec. VII is presented the experiment we have conducted, starting with the data acquisition and showing all the classifier we have used. In Sec. VIII are reported the results of our experiment. Finally, in Sec. IX we talk about the main contribution of our experiment and further analysis in the future. A schematic representation of our work is shown in Fig. 1.

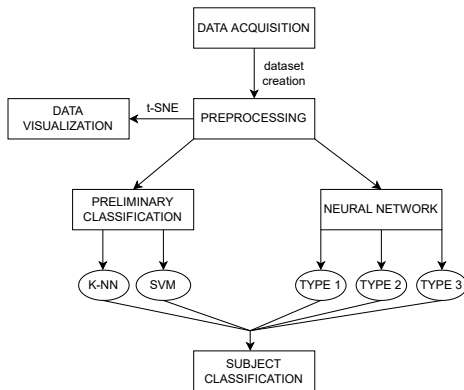


Fig. 1: Processing pipeline.

IV. METHODS

A. Preprocessing

The signals we acquire from the devices are subject to various types of noise. A preprocessing operation is necessary in order to clean the samples.

For the ECG signal, the main sources of noise are [17]:

- Baseline wander noise (0.1-0.5 Hz) (respiration, body movements, sweat, improper electrode connections).
- Power line interference (50/60 Hz) (interferences from electromagnetic fields of closing devices).
- Electromyogram noise (100 Hz) (shrinkage of muscles other than the cardiac muscles).

In our case, the only type of noise that we have is the first one, the baseline wander noise, as we can see from Fig. 2. Our signal, indeed, does not go over 40 Hz. Therefore we decided to apply a Butterworth highpass filter of order 8 [18] with cutoff frequency 0.5 Hz. The pulse oximeter is known to acquire a PPG signal that is more affected to noise than the ECG one. In our case (fingertip pulse oximeter), the noise is strictly correlated to the movement of the hand, to the breathing process, and so it is more personal and could carry useful information in the classification problem. We apply a Butterworth highpass filter of order 4 [4] with cutoff frequency 0.5 Hz.

Lastly, an appropriate scaling is done on the whole dataset using sklearn `StandardScaler` (removing the mean and scaling to unit variance).

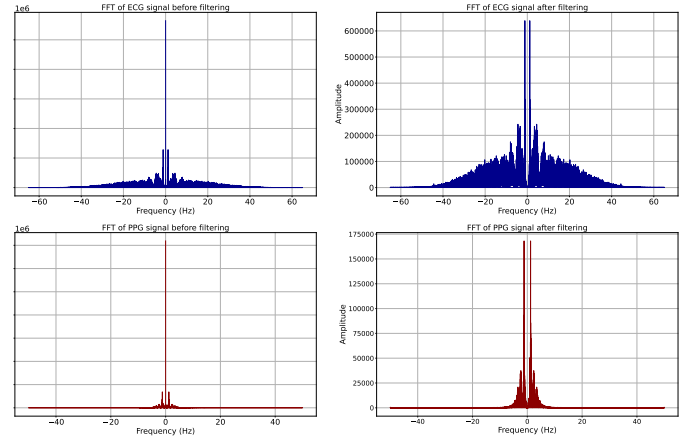


Fig. 2: FFT of signals before and after the filtering operation. In the top-left the non-filtered ECG signal, in the top-right the filtered signal. The same is shown for the PPG signal in the bottom part of the figure. The low-frequency noise is removed in both cases.

B. t-SNE

t-SNE is an algorithm that allows to visualize high dimensional data. These are projected into an 2 or 3 dimensional space. In our study, we use it in order to obtain a first idea of the dataset, to see how data are locally distributed. Indeed, t-SNE is a non-linearity dimensional reduction technique and

it tries to preserve the local structure of the data, whereas PCA preserves the global structure. It is important to notice that it is impossible to use t-SNE as dimensionality reduction technique for classification, because it does not learn a function from original space to the new one, so it can not map new points to the less-dimensional space.

C. *k*-NN

As first classification tool, the *k*-NN algorithm together with the Euclidean distance is used, since data shows local structure. In this way, we are able to see if the samples are automatically separated into clusters. The classification is done first using the original signal and then a less dimensional signal, achieved using PCA with 95% variance, both for the signal before and after the filtering operation.

D. SVM

Support vector machine (SVM) algorithm is suitable for high dimensional datasets, as in our case. It can perform a non-linear classification by mapping the inputs into a high-dimensional feature space. The main problem of SVM is the set of the parameters. Different types of kernel, degree (for poly kernels), regularization parameter, gamma parameter can be fixed. In order to reach the highest accuracy, a grid search on the parameters is performed on a set of different parameters.

E. CNN

A convolutional neural network is a translationally invariant neural network that respects locality of the input data. There are two kinds of basic layers that make up a CNN: a convolution layer that computes the convolution of the input with some of filters, and pooling layers that coarse-grain the input while maintaining locality and spatial structure. Often, as in the case of this work, the CNN is coupled with a Multilayers Perceptron (MLP): the former architecture is used as a features extractor and the latter is used for the classification task.

V. CNN ARCHITECTURES

In this work we have used three different Neural Network architectures, from now on we call it *Type I*, *Type II* and *Type III*. Given the nature of our signals *i.e.* samples of time series of fixed length, the idea behind this work is to create an algorithm that find peculiar patterns which belong to the subjects in our datasets, so we decide to use a convolutional neural network in order to extract features and then add at the end a Feedforward neural network in order to make inference. Following are shown the main characteristics of each architecture. The activation function for all the layers is the Relu, except for the last one: in that case we apply the SoftMax. We also use the Dropout regularization technique after the Maxpooling layers and the batch normalization in the convolutional layers.

1) *Type I*: this architecture (1151 trainable parameters) is composed in the following way:

- Conv1D(8, kernel_size).
- MaxPool1D(poolsize=2).
- Flatten layer.
- Dense(7).
- Dense(4).

2) *Type II*: it is the second neural network. In this case we have 1437 trainable parameters, and it is composed in the following way:

- Conv1D(8, kernel_size).
- Conv1D(8, kernel_size).
- MaxPool1D(poolsize=2).
- Flatten layer.
- Dense(5).
- Dense(4).

3) *Type III*: in this case we decide to create a more simpler neural network to make a comparison with the *Type I*: in this case we have 853 parameters. The architecture is the following:

- Conv1D(8, kernel_size).
- MaxPool1D(poolsize=2).
- Flatten layer.
- Dense(5).
- Dense(4).

VI. DEVICES

A. Pulse oximeter: LC_BM2000D by Abinrax

Pulse oximeter is a medical device that monitors the oxygen saturation and the changes on blood volume in the skin in a noninvasive way. These devices can measure the so called SpO_2 , *i.e.* an estimation of the oxygen saturation level, but in this work we use it to measure the changes on blood volume in the skin and to produce the so called photoplethysmogram (PPG). The change of volume is detected by illuminating the skin with light produced by a LED and then measuring the amount of light either transmitted or reflected to a photodiode. In our case we use the LC_BM2000D model of Abinrax, which work in a range of $25 \div 250$ BPM with an accuracy of ± 2 bpm and a resolution of 1 bpm. The typical PPG signal is shown in Fig. 3, whereas the one obtained by us with our sensor is shown in Fig. 4.

The pulse oximeter needs some second to stabilize before being able to record the data, and it is very sensitive to the motion of the hand. At rest, it is important to keep it motionless, but anyway our signals have different types of noise.

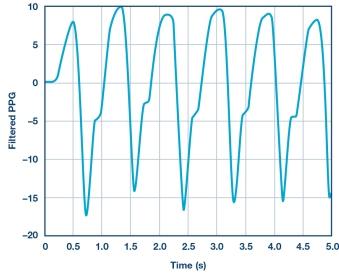


Fig. 3: Standard PPG wave.

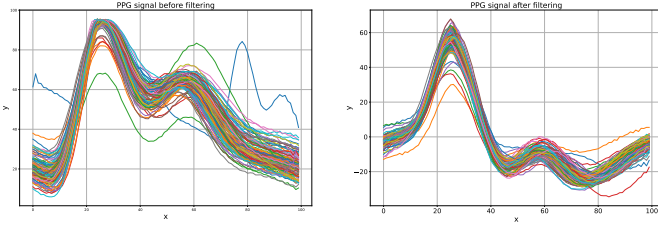


Fig. 4: Measured PPG wave. On the left before the filtering process, on the right after the filtering process.

B. ECG Sensor: POLAR H10

Electrocardiogram (ECG) is a graph of voltage versus time of the electrical activity of the heart using electrodes placed on the skin. These electrodes detect small electrical changes that are a consequence of cardiac muscle depolarization (P-wave) followed by repolarization (T-wave) during each heartbeat. A typical ECG graph of an heartbeat is reported in Fig. 5. The *POLAR H10* band is composed by an elastic band and two electrode, which have to be adherent between the thorax and the abdomen in order to record the data. Some samples of the ECG signal measured with our the band are shown in Fig. 6.

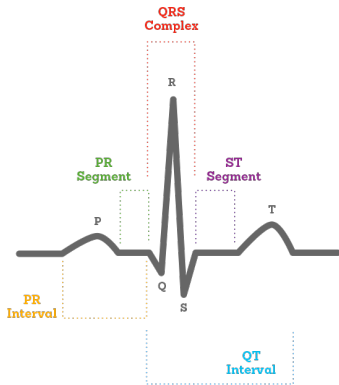


Fig. 5: Standard ECG wave.

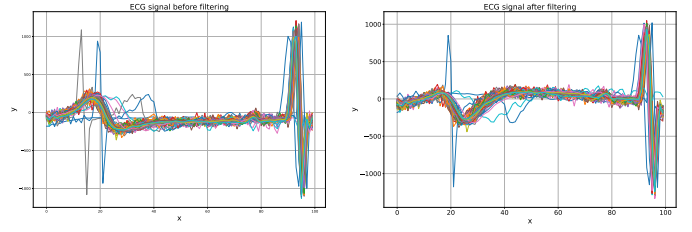


Fig. 6: Measured ECG wave. On the left before the filtering process, on the right after the filtering process.

VII. EXPERIMENTS

A. Dataset

Data have been taken using *pulse oximeter LC_BM2000D* and chest strap *Polar H10*, the devices have been worn at the same time and the data have been recorded simultaneously.

For the first dataset, we have recorded data from 4 different subjects sitting still (*at rest* dataset), whereas for the second dataset we have 2 different subject, but data have been taken both at rest and in motion (*in motion* dataset). At the end of the process, we have 2 different datasets divided each one in training set and validation set (20% of the whole dataset). Summary of the datasets are reported in Tab. 1 and Tab. 2.

Subject	N samples training set	N samples test set	% test set
A	2384	596	21.02%
B	3144	786	27.72%
C	3405	852	30.02%
D	2408	602	21.23%

TABLE 1: Summary of *at rest* dataset.

Subject	N samples training set	N samples test set	% test set
A at rest	2384	281	21.90%
A moving	1887	472	17.78%
B at rest	2557	639	24.10%
B moving	3844	962	36.22%

TABLE 2: Summary of *in motion* dataset.

B. Data visualization

Regarding the ECG signal, in Fig. 7 is reported the 2-D projection with perplexity parameter equal to 30 for both datasets. For the PPG signal, neither the 2-D and 3-D projections give a satisfying result: samples are mixed with each other and not easily separable.

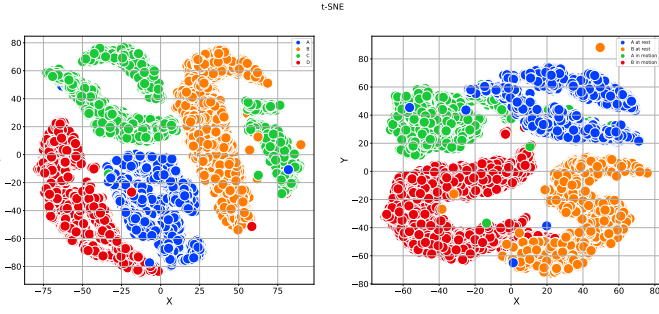


Fig. 7: t-SNE visualization for ECG signal. On the right the *at rest* dataset, on the left the *in motion* dataset.

C. Classification

K-NN and SVM are the first classification algorithms used. They are applied on both the original signal and the less dimensional signal (obtained using PCA algorithm), both for the signal before and after the filtering operation. This is done because we want to understand if it is possible to reduce the dimensionality of the dataset keeping high accuracy score, and how the filtering operation affects the dataset.

In order to tune the "free" hyperparameters of the CNNs, a grid search on the `Drop` and `kernel_size` is done. The values of the former are $[0.1, 0.2, 0.3, 0.4, 0.5, 0.6]$, whereas for the latter we choose $[2, 4, 8, 10, 16]$. We plot the accuracies of the grid search in a confusion matrix, shown in Fig. 8 as an example.

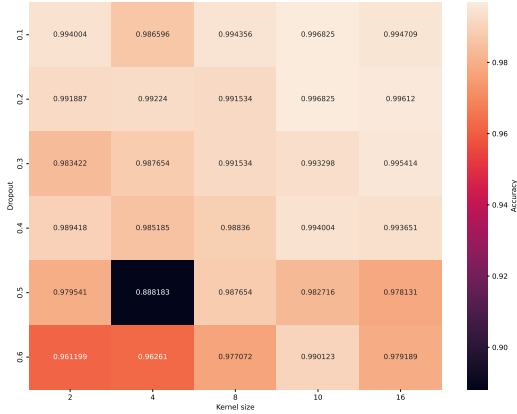


Fig. 8: Grid search on *Type I* for the filtered ECG signal.

1) **At rest dataset:** Accuracy of the k-NN algorithm for different value of k are reported in Fig. 9. For the latter, higher score are achieved using the non-filtered signal.

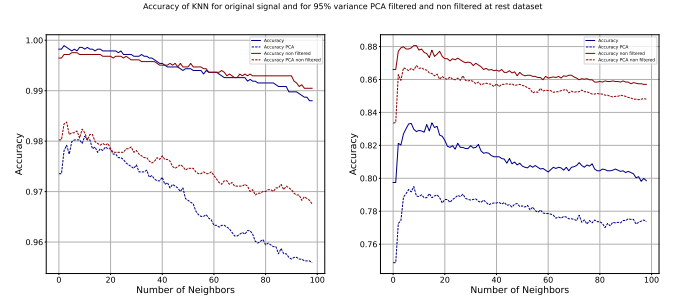


Fig. 9: K-NN algorithm accuracy comparison between original signal and PCA's output signal before and after filtering for *at rest* dataset. On the left the ECG signal, on the right the PPG signal.

Results of the CNNs are reported in Fig. 10 and Fig. 11. For the *Type I* architecture we have that the filtered and unfiltered signals both reach 99.68% accuracy on the test set, but the filtered signal converges 10 epochs before the other. Using *Type II* architecture we increase the complexity of the neural network, but this does not improve the performances, also in this case the filtered signal converges before the non-filtered one.

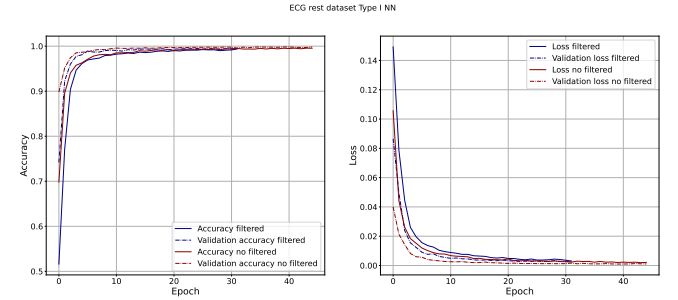


Fig. 10: *Type I* neural network accuracy and loss comparison between ECG signal before and after the filtering for *at rest* dataset.

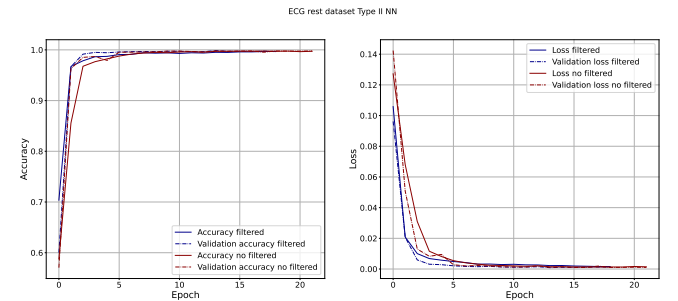


Fig. 11: *Type II* neural network accuracy and loss comparison between ECG signal before and after the filtering for *at rest* dataset.

2) **In motion dataset:** In this part of the project we add a complexity layer, now we have an "activity recognition" task,

from the AI point of view.

As before, in Fig. 12 are reported the accuracy score for different value of k for k-NN algorithm. In this case, the scores achieved after the PCA operation are higher than the one achieved before.

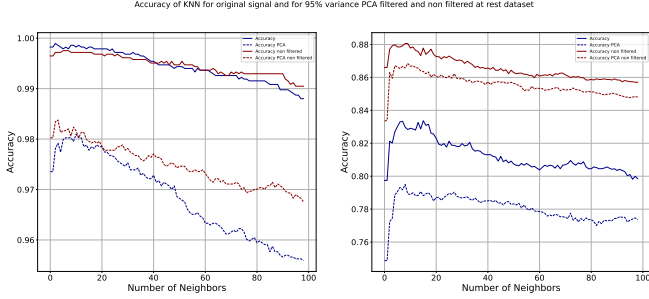


Fig. 12: K-NN algorithm accuracy comparison between original signal and PCA's output signal before and after filtering for *in motion* dataset. On the left the ECG signal, on the right the PPG signal.

Even if we have the same signals as before, we think to deploy the neural networks architectures of this section in a Bluetooth Low Energy (BLE) device, so we try to make the neural networks as small as possible. The idea is to reduce the number of parameters without a significant drop in performance. The results for the *Type I* architecture are reported in Fig. 13. We achieve an accuracy of 99.58% which is roughly the same as in the previous case. As shown in Fig. 14, for *Type III* architecture we achieve a high accuracy 99.5%. In this case the neural network needs more epochs to converge, but the results are nearly the same as before.

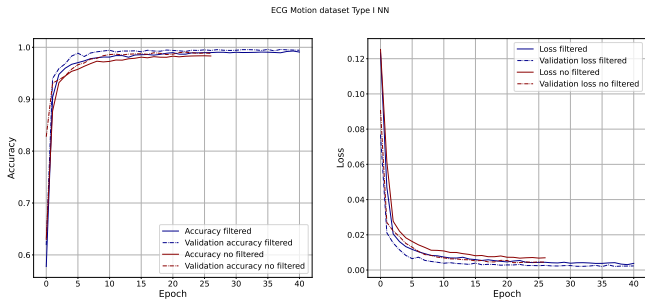


Fig. 13: *Type I* neural network accuracy and loss comparison between ECG signal before and after the filtering for *in motion* dataset.

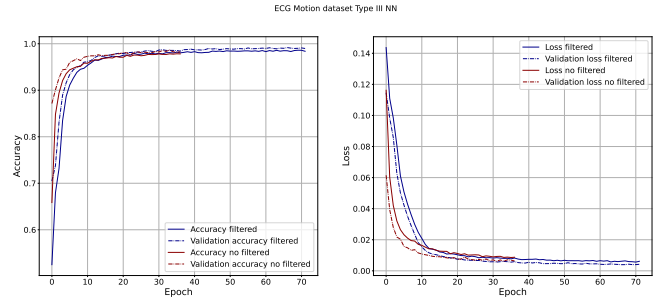


Fig. 14: *Type III* neural network accuracy and loss comparison between ECG signal before and after the filtering for *in motion* dataset.

VIII. RESULTS

Let's summarize the results achieved, starting from the data visualization. The t-SNE algorithm shows a relevant local structure of the ECG signal, as we can see from Fig. 7. This leads us to believe that we can achieve high accuracy in the classification task using density based algorithm such as k-NN and SVM. This is indeed what we obtain, as we can see from Tab. 3 and Tab. 4. The prediction of the test set accuracy are between 98% and 99% for both datasets.

For the PPG signal, the results achieved are worse. What is interesting to say is that the non-filtered signal leads to better results than the filtered one. This is probably due to the fact that the filtered noise is personal and relevant to perform an accurate classification. Indeed, since it is due to breathing motion, muscular motion, by filtering it we remove some personal characteristics that are not present in other subjects. A confusion matrix of the PPG signal for *in motion* dataset is shown in Fig. 15. We can see that the only label misclassified is *A moving* (that is considered as *B moving* for about 50% of the times), whereas the others reach a high accuracy. The confusion matrix is similar for every classification algorithm. This could be due to the fact that the samples of *A moving* were not well-taken or they have some intrinsically problem due to the devices or motion of the subject, or that the classification algorithm is not able to separate the *in motion* samples.

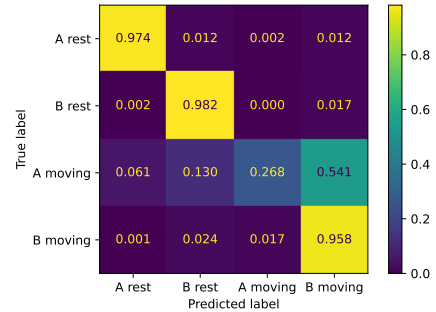


Fig. 15: Confusion matrix of PPG signal for *in motion* dataset, using k-NN algorithm.

Algorithm	ECG acc.	Time (s)	PPG acc.	Time (s)
K-NN	99.89%	0.003	83.36%	0.003
K-NN (PCA)	98.09%	0.001	79.49%	0.001
K-NN NF	99.75%	0.003	88.05%	0.003
K-NN NF (PCA)	98.37%	0.001	86.84%	0.001
SVM	99.92%	0.8	88.98%	6.7
SVM (PCA)	98.87%	0.5	88.98%	6.6
SVM NF	99.82%	0.7	86.70%	7.1
SVM NF (PCA)	99.08%	1.5	91.00%	5.9
Type I	99.68%	14.0	/	/
Type I NF	99.68%	14.7	/	/
Type II	99.68%	12.3	/	/
Type II NF	99.68%	17.3	/	/

TABLE 3: Highest accuracy score achieved for each algorithm and each type of signal, together with the computational time, for *at rest* dataset.

Algorithm	ECG acc.	Time (s)	PPG acc.	Time (s)
K-NN	97.92%	0.003	88.85%	0.002
K-NN (PCA)	98.26%	0.001	88.81%	0.001
K-NN NF	98.15%	0.003	89.80%	0.002
K-NN NF (PCA)	98.26%	0.001	89.39%	0.001
SVM	99.62%	0.8	90.14%	4.0
SVM (PCA)	99.24%	0.4	90.14%	4.0
SVM NF	99.66%	0.7	90.88%	4.3
SVM NF (PCA)	98.90%	0.2	90.88%	4.3
Type I	99.43%	12.5	/	/
Type I NF	99.58%	11.8	/	/
Type III	99.51%	13.2	/	/
Type III NF	99.43%	11.5	/	/

TABLE 4: Highest accuracy score achieved for each algorithm and each type of signal, together with the computational time, for *in motion* dataset.

A CNN approach has been tried on the PPG signals, but the architectures were too complex (about 400K trainable parameters) to achieve around 90% accuracy scores. We decide to not include that part in the project.

Regarding the ECG signal, the highest accuracy is reached using the SVM algorithm (for *at rest* dataset), and the k-NN algorithm (for the *in motion* dataset), both using the filtered signal. For the PPG signal, the best algorithm is the SVM for both datasets, applied to the non-filtered signal and after the PCA projection.

The third and fifth column of Tab. 3 and Tab. 4 report the computational time to train the classifiers, taken as a mean over 100 experiments. Our classification algorithm are extremely fast, especially for the ECG signal. This is an important result since in biometric authentication and identification is fundamental to have small computational time. The training of the k-NN is fastest one, whereas for the PPG signal we have a relevant difference between the computational time

of the k-NN and the one of the SVM (but the latter reach higher accuracy).

IX. CONCLUDING REMARKS

In our work we managed to construct two datasets that can be used to achieve optimal results in biometric subject identification, using two user-friendly devices. Moreover, the data were collected in a small amount of time and they only require simple fixed preprocessing operation. The accuracy score over the test set achieved are relatively high, especially the one obtained for the ECG signal.

What is important to say, is that these devices are able to record data in a continuous way, such that it is possible to enlarge and improve the accuracy of the model continuously, reaching more optimal results, making easier to identify more subjects. Also, it is necessary to investigate the accuracy reached using a smaller training set, because this would speed up the whole process. Moreover, even if ECG signal is more accurate than the PPG one, the latter is easiest to capture and less invasive. What is necessary to develop is more sensible devices for the PPG signal, less affected to noise due to motion and breathing processes. Also, a dataset made up by both the signal together could increase the performance of the network.

We decided to approach this task because we thought it would have been interesting to implement a biometric identification model from scratch, given only the devices and the software to records the data. By doing so, we have learnt how to construct a dataset, in particular how to setting up the process of data taken, how to choose the external conditions and the number of samples. In order to apply an appropriate filtering operation, we have studied filtering techniques applied on signals, which was new to us. This was indeed the main problem we have encountered, since our theoretical background was not useful in this application field.

REFERENCES

- [1] L. Li, C. Chen, L. Pan, J. Zhang, and Y. Xiang, "Sok: An overview of ppg's application in authentication," *CoRR*, vol. abs/2201.11291, 2022.
- [2] S. Hinatsu, D. Suzuki, H. Ishizuka, S. Ikeda, and O. Oshiro, "Photoplethysmographic subject identification by considering feature values derived from heartbeat and respiration," in *2020 42nd Annual International Conference of the IEEE Engineering in Medicine Biology Society (EMBC)*, pp. 902–905, 2020.
- [3] J. Sancho, Á. Alesanco, and J. Garc  a, "Biometric authentication using the ppg: A long-term feasibility study," *Sensors*, vol. 18, no. 5, 2018.
- [4] A. Sarkar, A. L. Abbott, and Z. Doerzaph, "Biometric authentication using photoplethysmography signals," in *2016 IEEE 8th International Conference on Biometrics Theory, Applications and Systems (BTAS)*, pp. 1–7, 2016.
- [5] J. Yang, Y. Huang, R. Zhang, F. Huang, Q. Meng, and S. Feng, "Study on ppg biometric recognition based on multifeature extraction and naive bayes classifier," *Sci. Program.*, vol. 2021, pp. 5597624:1–5597624:12, 2021.
- [6] T. Shen, W. Tompkins, and Y. Hu, "One-lead ecg for identity verification," in *Proceedings of the Second Joint 24th Annual Conference and the Annual Fall Meeting of the Biomedical Engineering Society [Engineering in Medicine and Biology]*, vol. 1, pp. 62–63 vol.1, 2002.
- [7] R. Donida Labati, V. Piuri, F. Rundo, F. Scotti, and C. Spampinato, "Biometric recognition of ppg cardiac signals using transformed spectrogram images," in *Pattern Recognition. ICPR International Workshops and Challenges* (A. Del Bimbo, R. Cucchiara, S. Sclaroff, G. M. Farinella, T. Mei, M. Bertini, H. J. Escalante, and R. Vezzani, eds.), (Cham), pp. 244–257, Springer International Publishing, 2021.

- [8] D. Biswas, L. Everson, M. Liu, M. Panwar, B.-E. Verhoef, S. Patki, C. H. Kim, A. Acharyya, C. Van Hoof, M. Konijnenburg, and N. Van Helleputte, "Cornet: Deep learning framework for ppg-based heart rate estimation and biometric identification in ambulant environment," *IEEE Transactions on Biomedical Circuits and Systems*, vol. 13, no. 2, pp. 282–291, 2019.
- [9] L. Everson, D. Biswas, M. Panwar, D. Rodopoulos, A. Acharyya, C. H. Kim, C. Van Hoof, M. Konijnenburg, and N. Van Helleputte, "Biometricnet: Deep learning based biometric identification using wrist-worn ppg," in *2018 IEEE International Symposium on Circuits and Systems (ISCAS)*, pp. 1–5, 2018.
- [10] J. Xu, T. Li, Y. Chen, and W. Chen, "Personal identification by convolutional neural network with ecg signal," in *2018 International Conference on Information and Communication Technology Convergence (ICTC)*, pp. 559–563, 2018.
- [11] M. Chourasia, A. Thakur, S. Gupta, and A. Singh, "Ecg heartbeat classification using cnn," in *2020 IEEE 7th Uttar Pradesh Section International Conference on Electrical, Electronics and Computer Engineering (UPCON)*, pp. 1–6, Nov 2020.
- [12] S. S. Abdeldayem and T. Bourlai, "Ecg-based human authentication using high-level spectro-temporal signal features," in *2018 IEEE International Conference on Big Data (Big Data)*, pp. 4984–4993, 2018.
- [13] G. Dingfei, "Study of ecg feature extraction for automatic classification based on wavelet transform," in *2012 7th International Conference on Computer Science Education (ICCSE)*, pp. 500–503, 2012.
- [14] D. Thanapatay, C. Suwansaroj, and C. Thanawattano, "Ecg beat classification method for ecg printout with principle components analysis and support vector machines," in *2010 International Conference on Electronics and Information Engineering*, vol. 1, pp. V1–72–V1–75, 2010.
- [15] Z. Ge, Z. Zhu, P. Feng, S. Zhang, J. Wang, and B. Zhou, "Ecg-signal classification using svm with multi-feature," in *2019 8th International Symposium on Next Generation Electronics (ISNE)*, pp. 1–3, 2019.
- [16] T. Li and M. Zhou, "Ecg classification using wavelet packet entropy and random forests," *Entropy*, vol. 18, no. 8, 2016.
- [17] K. K. Patro and P. R. Kumar, "De-noising of ecg raw signal by cascaded window based digital filters configuration," in *2015 IEEE Power, Communication and Information Technology Conference (PCITC)*, pp. 120–124, 2015.
- [18] A. Fedotov, "Selection of parameters of bandpass filtering of the ecg signal for heart rhythm monitoring systems," *Biomedical Engineering*, vol. 50, 09 2016.